# Biodistribution of Carbon Nanotubes in Animal Models

Jacobsen, Nicklas Raun; Møller, Peter; Clausen, Per Axel; Saber, Anne Thoustrup; Micheletti, Christian; Jensen, Keld Alstrup; Wallin, Håkan; Vogel, Ulla

*Published in:*
Basic & Clinical Pharmacology & Toxicology

*DOI:*
10.1111/bcpt.12705

*Publication date:*
2017

*Document version*
Publisher's PDF, also known as Version of record

BCPT Basic & Clinical Pharmacology & Toxicology

*Basic & Clinical Pharmacology & Toxicology*, 2017, **121**, 30–43 Doi: 10.1111/bcpt.12705

***MiniReview***

# Biodistribution of Carbon Nanotubes in Animal Models

**Nicklas Raun Jacobsen[1], Peter Møller[2], Per Axel Clausen[1], Anne Thoustrup Saber[1], Christian Micheletti[3], Keld Alstrup Jensen[1], Håkan Wallin[1,2] and Ulla Vogel[1,4]**

[1]The National Research Centre for the Working Environment, Copenhagen, Denmark, [2]Department of Public Health, Section of Environmental Health, University of Copenhagen, Copenhagen K, Denmark, [3]ECAMRICERT, Vicenza, Italy and [4]Department of Micro and Nanotechnology, Technical University of Denmark, Lyngby, Denmark

(Received 9 September 2016; Accepted 10 November 2016)

*Abstract:* The many interesting physical and chemical properties of carbon nanotubes (CNT) make it one of the most commercially attractive materials in the era of nanotechnology. Here, we review the recent publications on *in vivo* biodistribution of pristine and functionalized forms of single-walled and multi-walled CNT. Pristine CNT remain in the lung for months or even years after pulmonary deposition. If cleared, the majority of CNT move to the gastrointestinal (GI) tract via the mucociliary escalator. However, there appears to be no uptake of CNT from the GI tract, with a possible exception of the smallest functionalized SWCNT. Importantly, a significant fraction of CNT translocate from the alveolar space to the near pulmonary region including lymph nodes, subpleura and pleura (<7% of the pulmonary deposited dose) and to distal organs including liver, spleen and bone marrow (~1%). These results clearly demonstrate the main sites of long-term CNT accumulation, which also includes pleura, a major site for fibre-induced pulmonary diseases. Studies on intravenous injection show that CNT in blood circulation are cleared relatively fast with a half-life of minutes or hours. The major target organs were the same as identified after pulmonary exposure with the exception of urine excretion of especially functionalized SWCNT and accumulation in lung tissue. Overall, there is evidence that CNT will primarily be distributed to the liver where they appear to be present at least one year after exposure.

Amongst the many interesting materials refined in the era of nanotechnology, carbon nanotubes (CNT) are one of the most celebrated and technically attractive manufactured nanomaterials to date. They are frequently praised as the new wonder material of nanotechnology. These nanometre-thin hollow tubes, with their lightness, conductivity and extreme strength and stability, have shown many promising properties within material science, coatings, electronics, as well as biomedicine; and they are already used in a number of materials and products [1]. It appears without question that material scientists will generate new possibilities with CNT as well as will improve a variety of industrial, consumer and medical products. Everything from reinforcement of skyscrapers to clothes, from electronics to drug delivery, is envisioned.

Several companies have engaged in commercial scale production or utilization of CNT, and they are available worldwide. The global market for CNT products was estimated to reach a trade value of 2.26 billion in 2015 and to reach USD 5.64 billion by 2020 [2]. The rapid increase is explained by both the extraordinary properties by CNT and the increasing ability to mass-produce at commercially attractive prices.

A rapid increase in production and products inevitably leads to increased occupational, consumer and environmental exposure. As for many other nanomaterials [3,4], this has raised concerns for CNT, especially because they have physical traits similar to asbestos [5]. Asbestos was previously praised as a wonder material, but exposure has since been shown to increase the risk of developing mesothelioma, lung cancer, asbestosis, pleural plaque and effusion [6]. The most important similar characteristics between CNT and asbestos are the very poor solubility and their fibrous morphology with some CNT materials having a long, rigid needle-like appearance (high aspect (length over diameter) ratio). Consequently, CNT longer than 5 μm are thus in compliance with the WHO fibre paradigm. Such fibres are thin enough to be inhaled and reach the alveolar region, long enough to evade phagocytic engulfment and highly biopersistent [5]. These characteristics make pulmonary toxicity and further translocation to, for example, the pleura possible for an extended period of time.

Such concerns are a natural impediment to widespread technological use of CNT and toxicological results have so far not eased the concern that at least some CNT may be able to induce serious human health effects [7–9]; especially, the two OECD guideline studies by Ma-Hock *et al.* and Pauluhn [10,11] have been noticed with results clearly showing prolonged pulmonary inflammation and granulomas. Less effect was observed at lowest tested dose (0.1 mg/m$^3$), and this was suggested as the no observable effect level (NOEL). For the latter study, 0.05 mg/m$^3$ was suggested as occupational exposure limit (OEL) [12].

Author for correspondence: Nicklas Raun Jacobsen, The National Research Centre for the Working Environment, Lerso Parkalle 105, DK-2100 Copenhagen, Denmark (e-mail nrj@nrcwe.dk).

The most studied CNT (MWCNT-7/XNRI-7) has been categorized as possible carcinogenic to human beings by International Agency for the Research on Cancer (IARC) as group 2B. All other CNT are not yet classifiable due to limited toxicological research [9]. However, recent publications show that the profile of the overall global transcription and the acute phase response was very similar after pulmonary exposure in mice to two multi-walled carbon nanotubes (MWCNT) with quite different dimensions (short L:0.9 μm, D:11 nm; long 4.1 μm, 67 nm) [13,14]. Additionally, a high degree of concordance was also observed when comparing global transcription profiles to those of MWCNT-7 [14,15], indicating that more research may lead to further CNT being classified by IARC. Using a battery of 10 commercial MWCNT, the same group also identified BET surface area as a predictor for pulmonary inflammation, but inversely correlating with genotoxicity in BAL cells and lung tissue. This indicates that thicker MWCNT may cause less inflammation, but more genotoxicity [16].

Despite these toxicological considerations, carefully tailored CNT are still highly interesting for nanomedicine (drug delivery, targeting, visualization, etc.) as they possess some unique characteristics leading to possibilities that may outweigh the challenges and toxicity. Some can absorb a wide spectrum of light and emit near-infrared (NIR) light traceable with low interference in biological tissues. If irradiated with NIR light, CNT produce heat that could be used for killing nearby cells. They are stable even in harsh environments, which means safe passage to targeted cells for materials loaded in the core. If the CNT are surface-modified to hydrophilicity, this could include a load of highly hydrophobic chemicals [17].

## Content and Aims

In the present MiniReview, we discuss up-to-date knowledge of *in vivo* biodistribution of CNT. As translocation is the most likely hypothesis to explain toxicity at sites distal from entry, it is critical information for a hazard evaluation. By identifying tissues where CNT accumulate, tissues with potential target effects are also identified. Therefore, the biodistribution is described and evaluated after all exposure routes: inhalation or other pulmonary deposition methods; oral gavage and uptake through the GI tract; distribution after IV and peritoneal deposition. Both single-walled (SWCNT) and multi-walled carbon nanotubes (MWCNT) (pristine and functionalized) are included in this MiniReview. Finally, as many different CNT detection methods have been used, greatly varying in sensitivity and reliability, results are discussed based on the views of the authors of the present paper on the reliability of the methods.

## Search Strategy and Selection of Studies for the Review

Publications were identified by PubMed and Google Scholar searches by use of combinations of keywords for the material (i.e. carbon nanotube, multi-walled carbon nanotube, single-walled carbon nanotube, CNT, SWCNT, MWCNT, SWNT, MWNT), methods (i.e. biodistribution, distribution, pharmacokinetics, kinetics) and species (i.e. *in vivo*, animal, mice, mouse, rat rats, rabbit and rabbits). The abstracts were screened for information regarding experimental results on biodistribution of CNT. Overall searches using combinations of several keywords tended to under-report many studies (e.g. approximately 235 publications were identified in PubMed using the terms above). Thus, more simple searches were also used as well as specific searches on authors of identified publications. The publications were included after a critical assessment of the methodology (see later section on measurement of CNT in tissues) and transparency of the published results. Publications on experiments where CNT were modified for specific targeting (e.g. tumour targeting) were not included. Publications where translocation was identified, but not attempted quantified, have not been included in the review either. This MiniReview encompasses only publications on animal studies.

## Structure of Carbon Nanotubes

Carbon nanotubes comprise a highly variable group of hollow fibrous materials, which generally are depicted with either a single-walled (SW), double-walled (DW) or a multi-walled (MW) graphene-like tube (fig. 1). As implied by the name, SWCNT consists of a monolayer of a seamless rolled sheet of graphene. DWCNT and MWCNT consist of two and more of such rolled and stacked sheets of graphene. The diameters and lengths are typically in the range of 0.7–2.5 nm and 0.5–50 μm, 1.3–5 nm and 0.5–40 μm, 4–150 nm and 0.5–150 μm, for SW, DW and MWCNT, respectively [1]. Further variability and complexity is added by the presence of various impurities, levels of purification, rolling angle and chemical functionalizations. The apparent large variability in CNT types and purities makes it uncertain whether CNT, from a regulatory point of view, can be considered as one material at all or they should be grouped according to selected physical and chemical characteristics.

## How do CNT Enter the Human Body?

For hazardous particulates or fibres to affect human health, they must be internalized by inhalation, ingestion or injection. The highest unintentional CNT exposure will occur in occupational settings where CNT are produced, harvested, purified, functionalized, mixed and bagged. Although CNT exposure is negligible in the closed-reactor synthesis procedures, a particle/dust concentration (CNT and other) of 286 $\mu g/m^3$ has been measured during harvesting [18]. Up to 332 $\mu g/m^3$ (CNT and carbon black) have been observed during handling of CNT after opening a blender mixing composites in an unventilated area [19]. In occupational settings, the most important exposure route will be via inhalation and to a much lesser extent dermal contact. Ingestion will occur as a secondary consequence of swallowing fibres cleared from the pulmonary system via the mucociliary escalator. Additionally, an exposure could occur via hand-to-mouth contact.

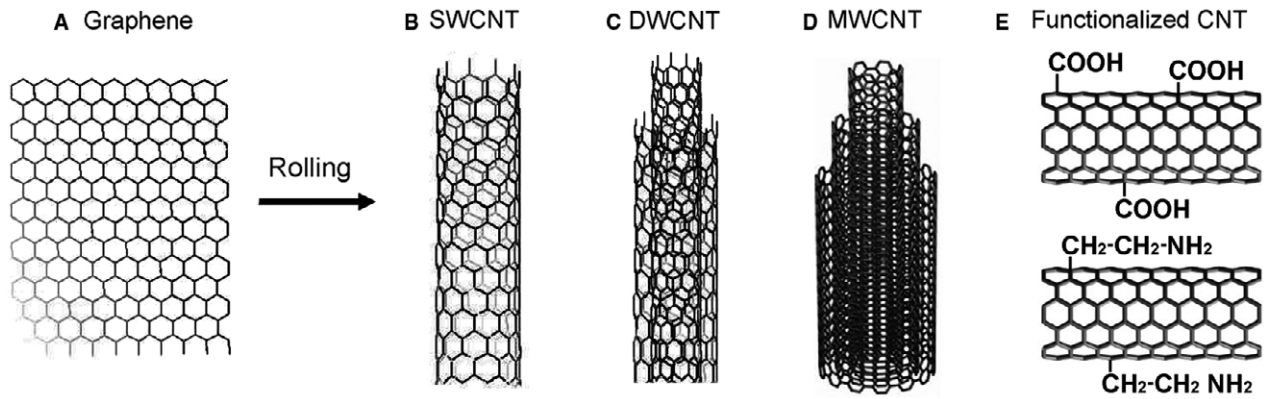


Fig. 1. Illustration of graphene (A) rolled up and welded into a seamless cylindrical single (B), double (C) or multi-walled (D) carbon nanotube. Possibilities are endless for surface modifications. Illustrated are carboxylation and amine functionalization (E). SWCNT, single-walled carbon nanotubes; DWCNT, double-walled carbon nanotubes; MWCNT, multi-walled carbon nanotubes. Reprinted with permission from Chemistry Central [8].

Carbon nanotubes are envisioned in nanomedical applications such as imaging, drug delivery and gene therapy. Such deliberate exposure would likely take place via ingestion, subcutaneous or IV/IP injection. However, as much remains unknown about the transport mechanisms, fate and especially adverse health effects of CNT, a biomedical/nanomedicine application of CNT is not believed to reach the market in the near future. Also, as discussed in [17], we still have not seen 'any real-life biotechnological CNT breakthrough justify taking these materials forward into the clinic'.

## How is CNT Measured in Tissue?

*Direct detection.*
Carbon nanotubes are difficult to detect visually in tissues unless they occur in large agglomerates. It is time-consuming to identify CNT and especially to give a semi-quantitative estimate of the deposited dose. However, a direct identification or visualization is highly important as it eliminates many of the uncertainties coupled to indirectly measured CNT by chemical or physical analysis of tracers.

*Microscopy.* Light and especially electron microscopy are popular methods to demonstrate the presence of CNT in tissues. It is often used to support other detection techniques. Detection of CNT may be a major challenge in secondary exposed organs where minimal mass concentrations are expected. However, when detected, the special structure of CNT is often easily identified, although certain cellular structures (crystalline bodies caused by eosinophilic crystalline pneumonia) closely resemble CNT [20]. A recently developed technique is hyperspectral microscopy, which identifies nanomaterials based on their signature refractive index [21]. This enables an easier identification of CNT in tissues. As with all microscopic techniques, it is limited to a qualitative detection of CNT. In order to make it semiquantitative, Mercer *et al.* performed an approach by extrapolating the amount of CNT detected in five scored slides to whole organs. Although such scores come with large uncertainties, they are important as they represent a direct identification of CNT in tissues.

*Raman.* Raman spectroscopy can identify CNT via the characteristic inelastic scattering of laser light. It is able to detect both agglomerated and individual CNT [22]; especially, it has been used in a range of studies for the detection of SWCNT [23–27]. However, even though the specificity is high, the sensitivity is not always sufficient. One reported a detection limit of 0.04 μg/ml blood (0.2% of the dose/g) and 0.2 μg/ml (1% of the dose/g) in homogenized and solubilized tissues [24]. Others report higher detection limits. Additionally, changes to the CNT structure may weaken the signal intensity and render the material impossible to detect in tissue slides. Such structural damage of CNT will likely occur during longer *in vivo* studies and will lead to detection being less quantitative.

*Near-infrared fluorescence.* The use of near-infrared (NIR) fluorescence is in general a promising way of detecting SWCNT or other markers *in vivo*. The most useful of detected wavelengths (emitted after laser excitation) for SWCNT are 700–900 nm or around 1100–1400 nm. These are often termed 'the biological transparency windows' due to low optical scattering, low autofluorescence and low absorption from haemoglobin and water in tissues. This has been used both in tissue sections and in microscopic preparation to detect bulk SWCNT or individual SWCNT [28]. Signal intensity does decay with tissue depth, but it has been shown that SWCNT can be detected several millimetres inside tissue [29].

*Indirect detection.*
For the detection sensitivity of CNT in tissues, radiolabelling methods are better than Raman spectroscopy, NIR fluorescence and microscopy. However, as sensitivity increases, the

reliability often decreases. The stability of the labelling should be determined over time in a harsh and realistic biological environment (fig. 2).

*Radioactivity and metal tracers.* Many different radiotracers exist and are used as a proxy for the detection of CNT. The best are the skeleton $^{13}$C-enriched SWCNT used by Yang *et al.* [30] and especially radioactive $^{14}$C MWCNT used by Czarny *et al.* [31]. Both have the $^{13}$C or $^{14}$C as part of the atomic CNT structure and the activity can thus not detach from the CNT. Biodistribution was detected via isotope ratio ($^{13}$C/$^{12}$C) mass spectroscopy. However, the relatively high presence of $^{13}$C in biological tissues (~1.1% of C) affects the sensitivity of the technique. The detection limit was reported to be 1 μg/g tissue by Yang, which makes the detection of smaller deposited doses difficult. This was alleviated by use of $^{14}$C. Czarny *et al.* [31] demonstrated a very strong radioactive signal, which was accomplished by a ratio of 1/17 ($^{14}$C/$^{12}$C) in the MWCNT. The detection limit was reported to be 0.2 pg, equivalent to 22 intact CNT in tissue samples [31].

Another study used MWCNT with $^{14}$C bonded covalently directly to the surface of the tube. As the C-C bond is extremely strong and situated in as close proximity to the tube as possible, this radioactive label appears highly robust. The detection limit of 10 pg was also relative low [32]. Others have used radiolabeling located at similar distance from the CNT, using weaker covalent bonds (dissociation energy) ($^{125}$I-taurine-, $^{125}$I-Tween-MWCNT) [33,34]. The size and nature of iodine makes the C-I bond much more labile than the C-C bond, which increases the risk for radioactive iodine ions being detached from the CNT lattice structure. Another approach has been to load isotopes ($^{125}$I) or metal tracers (Ni, Gd, Pt) inside or on the tube [35–37]. Again, the chemical bond to the tube is important. In one paper, a detection limit of 0.01 μg/ml (mineralized acid-treated tissue) of Ni was mentioned. However, as 0.53% Ni (w/w) was in the CNT, it does not allow for the detection of smaller fractions of translocated material.

It is of great concern that as distance between CNT and tracer increases so does the possibility of detachment of tracer. This may lead to a biased quantification of CNT in tissue samples because of detection of free radiotracers. Examples of larger constructs and long distance between tracer and tube are $^{14}$C-taurine [38], $^{99m}$Tc linked to MWCNT via glucosamine [39]. A large number of publications have used radiotracers, which have been anchored to larger molecules such as diethylene-triamine-penta-acetic-acid dianhydride (DTPA) or 1,4,7,10-tetraazacyclododecane-1,4,7,10-tetraacetic acid (DOTA) by a co-ordination (complex) bond. These complexes are attached to the CNT surface (fig. 2). As radiotracers, $^{111}$In [40–47], $^{64}$Cu [48] and $^{86}$Y [46,49] have been used in these constructs. It is very likely that such constructs are stable *ex situ*, but stability may be strongly reduced by the complex *in vivo* milieu. Table 1 summarizes the strengths and weaknesses of the discussed methods for detecting CNT in tissues. It should be noted that all methods (except structurally build-in detection of CNT and to a certain extent microscopy) suffer from the possibility that the structure of CNT may change over time releasing tracers or decreasing measured signal.

## Biodistribution

With the great potential of CNT products, it is vital to determine the biodistribution, persistence and clearance of CNT as part of a hazard characterization. Below is a presentation of

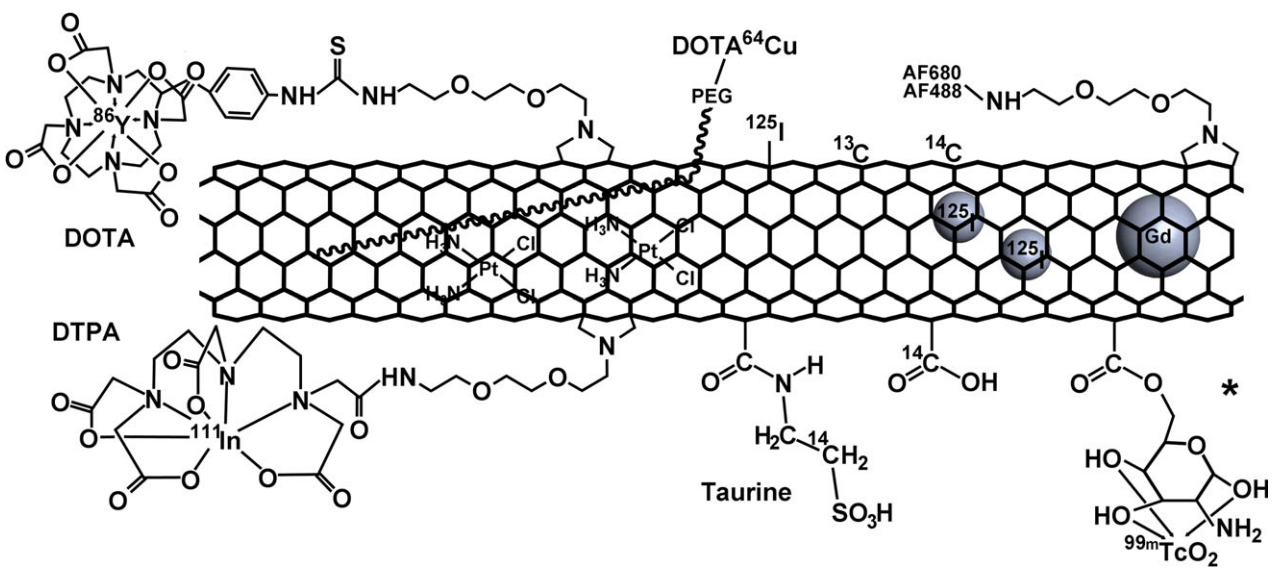


Fig. 2. Examples of the various indirect detections of SWCNT/MWCNT. The illustration is based on drawings and/or descriptions in the below-mentioned biodistribution papers. AF488 and AF680 are Alexa flour fluorophores. DOTA, 1,4,7,10-tetraazacyclododecane-1,4,7,10-tetraacetic acid; DTPA, diethylen-triamine-penta-acetic dianhydride. There are different examples of how DOTA and DTPA are attached to the CNT and of which tracers are used. *Our proposed structure (of several possibilities) for $^{99m}$Tc-glucosamine-MWCNT used by [39].

*Table 1.*

Detecting CNT in biological tissues with various methods.

| Methods | Specificity | Sensitivity | Quantitative | Comment |
|---|---|---|---|---|
| Microscopy | High–Medium | Low | No-semi | Difficult to detect. Misinterpretation |
| Raman | High | Medium | Semi (Yes) | Poor signal-to-noise ratio |
| NIR fluorescence | High | Medium | Semi (Yes) | Signal decreases strongly with depth |
| Radioactivity | | | | |
| Skeleton-enriched | High | High–Medium | Yes | Radioactivity cannot detach from the tube |
| Small constructs | High–Medium | High–Medium | Yes | The strength of the covalent bond to the CNT |
| Large constructs | High–Medium | High–Medium | Yes | The strength of the entire construct |
| Metal tracers | High–Medium | Medium–Low | Yes | The attachment and mass of the tracers |

Specificity is the ability of a method to correctly identify CNT from a signal. Sensitivity describes the chance of detecting small concentrations.

the original literature on biodistribution of CNT from primary deposition in airways, gastrointestinal tract, the bloodstream and the peritoneum. All discussed papers are summarized in table S1.

*Inhalation and instillation (and biological persistence).*

Inhalation is the major exposure route for particles. It has been shown that inhaled CNT have a very long pulmonary half-life (months to years) and thus persist in the alveoli and lung tissue long after exposure [12,35,50,51]. This means that translocation to circulation may occur for months or even years and extrapulmonary effects may increase or even arise long after exposure has ended.

Ryman Rasmussen *et al.* showed that inhaled MWCNT (L:0.5–40 μm, D:10–50 nm, 1 or 30 mg/m$^3$ for 6 hr) translocated to the subpleural region of the lung. CNT translocated rapidly (1 day) and were observed in the subpleura until the end of the experiment 14 weeks after exposure. CNT were observed both within macrophages, within subpleural mesenchymal cells and within the collagen matrix of the subpleura. The observations suggest migration of CNT as engulfed cargo within macrophages [52].

In line with this, Mercer *et al.* show that 0.6% of the pulmonary deposited dose after pharyngeal aspiration had translocated to the subpleura by day 1. The authors documented that MWCNT (Mitsui, XNRI MWNT-7, L:3.9 μm, D: 49 nm) penetrations of alveolar macrophages, the alveolar wall and visceral pleura were very frequent and sustained. They estimated that a pulmonary dose of 40 μg caused in excess of 20 million cellular penetrations throughout the lung and that 56 days post-exposure one of 400 fibre penetrations will be in the subpleural or intrapleural space [53].

Another study by the same group identified MWCNT (Mitsui, as above) inside as well as protruding from alveolar macrophages. Many of the penetrations went completely through both the cell and the cell nucleus. One hour after pharyngeal aspiration, MWCNT were engulfed by macrophages and by type 1 alveolar epithelial cells. At later time-points, MWCNT were not observed on the surface of epithelial cells, but were located within the alveolar interstitium, interstitial cells or alveolar macrophages. MWCNT were detected within the pleura 56 days post-pharyngeal aspiration [54]. Cellular penetrations have also been confirmed in mice studies of intratracheal instillation of short, tangled and long, thick CNT. Using several EM techniques, both tubes were observed both freely and inside vesicles in the cell cytosol. CNT were, however, never observed inside the nucleus [20,55].

A recent review by Donaldson *et al.* argued that this migration into the intrapleural space is common for a smaller fraction of all particles deposited in the distal lung. A suggested mechanism of particle clearance from the pleura is that particles follow lymph fluid through narrow holes (stomata) in the parietal pleura. However, the long fibres cannot migrate through the small stomata, leading to retention, local inflammation and pleural pathology, for example mesothelioma [5].

It should be underlined that the above publications only focused on intrapulmonary translocation and made no attempts to assess a further translocation to extrapulmonary organs. However, others have detected such a translocation. Ingle *et al.* detected a direct Raman signal of the inhaled unmodified SWCNT in the blood of mice [22], thereby showing the possibility of secondary organ exposure. They did not detect whether the CNT were excreted or accumulated.

Lin *et al.* detected the vast majority of instilled $^{125}$I-SWCNT in trachea and the GI tract, suggesting mucociliary clearance. However, small amounts (0.02–0.12% of the dose/g tissue) were detected in 16 other tissues.

In another study, translocation of 10 μg taurine-functionalized-MWCNT labelled with $^{14}$C (L: 10–600 nm, D: 10–15 nm) was followed after instillation in mice [38]. The instilled $^{14}$C-tau-MWCNT was only detected in the lungs, declining from 78% of the administered dose at day 1–20% at day 28. No $^{14}$C activity was detected in blood or key organs such as liver, spleen, kidneys, at any of the post-exposure time-points. However, the specific activity of the administered $^{14}$C-tau-MWCNT was 2700 cpm/μg; thus, the level of radioactive labelling might be too low to detect translocation in the order of a few per mille, which would be an expected level.

After instillation of 200 or 550 μg unmodified MWCNT, about 30% was cleared within 24 hr. The remaining 70% (120–150 μg and 280–380 μg, respectively) remained in the lung throughout 1 year with no indications of reduction. Tubes were not detected in liver or brain, but were detected in peribronchial lymph nodes [50]. Elgrabli *et al.*, [35] also

detected a translocation of Ni associated with the pristine MWCNT to the lymph nodes of rats (1, 10, 100 μg; L: 0.5–2 D: 20–50 nm). But in contrast to Shinohara, they found the lung burden continuously decreasing; 63–78% of the instilled Ni was detected in the lung at days 1, 7 and 30. After 3 months, 38% of the Ni was detected in the lung, and after 6 months, 16% was still detected in the lung [35].

Mercer *et al.* exposed mice for MWCNT aerosol (5 mg/m$^3$, 5 hr/days, 4 days/week for 3 weeks) and observed that all analysed tissue contained MWCNT, albeit in small amounts. The major extrapulmonary site was the tracheobronchial lymph nodes, which were found to contain 1 and 7% of the lung burden (28 μg) at 1 day and 336 days post-exposure, respectively. All other analysed tissues, liver, kidney, heart, brain, chest wall and diaphragm, contained ≤0.004% or ≤0.027% of the pulmonary dose at day 1 and day 336, respectively. The CNT were detected directly via light microscopy and hyperspectral imaging [21].

Czarny *et al.* [31] used pharyngeal aspiration to deposit 20 μg $^{14}$C skeleton-labelled MWCNT (L: 3.9 μm, D: 40 nm). Radioimaging showed that the pulmonary radioactivity decreased from 100% to 10% over 3 months. In the same time, small amounts of MWCNT translocated to distant organs with a clear increase over time. An increase in liver, spleen, kidney and bone marrow was observed from day 7 to day 360. Liver and spleen contained about 0.8% and 0.2% of the exposed dose, respectively, 1 year after exposure. Kidney and bone marrow contained much less <0.2% of the pulmonary dose. A possible secondary uptake from the GI tract was eliminated, as no translocation to spleen and liver was observed after an oral exposure (50 μg). The authors concluded that the observed translocation after lung exposure occurred through the pulmonary epithelium only [31].

Biodistribution may be affected by specific biological durability and degradation. In one study, SWCNT (not specified) were chemically cut [56] by sonication in $H_2SO_4$ and $H_2O_2$ to create short SWCNT that were carboxylated at both ends. These SWCNT could be degraded *in vitro* by a combination of human myeloperoxidase and $H_2O_2$. While aspiration of 40 μg/mice of the chemically cut SWCNT induced inflammation 24 hr after pharyngeal aspiration, degraded SWCNT did not cause inflammation. This indicates that the extent to which the CNT are biodegradable is a major determinant of the inflammatory response.

In summary, the above studies show that the majority of the deposited dose remains in the lung or is cleared towards the GI tract. However, a significant fraction appears to translocate to the near pulmonary region including subpleura/pleura (below 1%), lymph nodes (up to 7%) and to distal organs including liver and spleen of approximately 1% of the deposited dose. For the translocation to distant organs, we add great value to Czarny *et al.* [31]. The study design was valuable with strongly radioactive skeleton $^{14}$C-enriched MWCNT, allowing for the detection of ≥22 intact CNT in tissue samples [31]. Translocation was much higher than previously estimated (~0.03% of the pulmonary dose was estimated to be in the liver at day 336) [21]. The dose was estimated from results of semiquantitative hyperspectral microscopy. The spleen was not examined. It should be noted that Czarny *et al.* conducted a pharyngeal aspiration study, whereas Mercer's group conducted an inhalation study. However, it should also be noted that about 20% of the aspirated dose was still present in the lung 1 year post-exposure, and accumulation in lung and spleen could thus continue for even longer [31].

*Oral.*

It is well known that one mechanism of clearing particles from the pulmonary region is via the mucociliary escalator into the gastrointestinal tract for excretion via faeces. However, such transport upwards to the pharynx will lead to the particles being swallowed for a pass through the GI tract and a second possibility for systemic translocation through the intestine. This translocation occurs after all pulmonary exposures with a post-exposure time longer than a few hours.

Only few studies have attempted to determine biodistribution via the oral route. Heifang Wang *et al.* showed that small hydroxylated SWCNT ($^{125}$I-labelled KOH-SWCNT, L: 300 nm, D: 1.4 nm) could easily distribute to organs and compartments and basically moved freely and rapidly around the body despite a large molecular weight of 600 kDa. Three hours after oral administration of 1.5 μg, the SWCNT ($^{125}$I activity) were detected in all 12 analysed organs with highest concentrations in stomach, kidney, lungs and bone and with lowest concentrations in brain, heart and muscle [57].

Agglomerates of SWCNT (160 nm) with embedded gadolinium (Gd) nanoparticles did not show any signs of uptake after oral administration (2 mg/mouse). Gd was detected throughout the GI tract, but was not detected in blood, liver or spleen. About 80% was excreted within 8 hr and almost 100% within 24 hr [37].

Deng *et al.* studied distribution after 10 μg orally dosed small MWCNT ($^{14}$C-tau-labelled, L: 10–600 nm, D: 10–15 nm). These were detected in stomach, small intestine and large intestine, ending up in faeces. Radioactivity passed downstream over time. About 74% of the administered dose was excreted in faeces within 12 hr post-exposure. No labelling was detected in blood, indicating that $^{14}$C-tau-MWCNT was neither absorbed from the gastrointestinal tract nor entered the blood circulation in detectable concentrations [38].

Czarny *et al.* [31] detected translocation to various organs after lung deposition of $^{14}$C-enriched MWCNT. To determine the route of translocation, they performed an oral exposure study (50 μg; L: 3.9 μm, D: 40 nm). Twenty-four hours post-exposure, 95 ± 15% of the dose was found in the GI tract and faeces, and no radioactivity was detected in the GI tract and faeces from 4 days post-exposure. No radioactivity was detected in spleen and liver [31].

There are huge differences in biodistribution between these studies of ingested CNT, from no biodistribution to complete availability in all tested organs. Besides the differences in tracer and detection techniques used, the blatant disparity may be due to the size and shape of the tubes presented to the GI tract. The tubes had somewhat similar length, but not only

were the MWCNT used by Deng *et al.* about 10 times thicker, they also had a more flexible appearance than the straight needle-shaped SWCNT used in Heifang Wang's study (fig. 3). The tubes used by Nakamura were about 3 nm in diameter and 70 nm in length, but were 160-nm agglomerates in the exposure suspension (distilled water). Translocated tubes would only be detected if Gd also translocated.

Even though size may be important, it should be mentioned that SWCNT were detected indirectly via $^{125}$I. In order to strengthen that the free distribution of SWCNT was not caused by $^{125}$I alone, the authors showed that no unbound $^{125}I^-$ ions were adsorbed to the surface of the SWCNT. Additionally, a somewhat different distribution profile was observed for Na $^{125}$I compared to $^{125}$I-SWCNT. This led the authors to conclude that the observed biodistribution was of $^{125}$I-SWCNT and not $^{125}I^-$.

Overall, with one exception, there appears to be no obvious tissue uptake from the GI tract of CNT. The same has been observed previously with other nanomaterials such as $^{125}$I–graphene [58] and several $TiO_2$ materials [59].

*Biological distribution from blood (IV exposure).*
Nanomedicine may completely transform and revolutionize health care, and CNT make their mark within this field. Thus, it is not surprising that there are several publications on biodistribution of CNT after IV injection. However, it is of paramount importance that the pharmacokinetics and biological effects of promising candidates are fully understood before ideas are propelled to the development of medical agents. These studies mainly serve as examples of biodistribution of CNT translocating from the lung to systemic circulation. However, in the case of larger agglomerates being present in the exposure, it should be noted that after IV injection, the first capillary network encountered will be the pulmonary system.

*Unmodified CNT.* $^{13}$C-enriched SWCNT (L: 2–3 μm, D: 10–30 nm (bundles)) were injected in the tail vein and biodistribution was studied up to 28 days [30]. The authors excluded elimination via urine, but mentioned that very little excretion could be determined in faeces. Therefore, the pristine SWCNT were suggested to mainly be distributed and remain internally. $^{13}$C was detected in a variety of organs, with highest concentrations in the liver (21, 18 and 21% of the dose, respectively, after 1, 7 and 28 days), lung (15, 13 and 9% of the dose, respectively) and spleen (1, 2 and 2% of the dose). In the liver, SWCNT were localized in Kupffer cells as shown by electron microscopy. SWCNT were also detected in the lungs by TEM [30]. Unique for this study was the employment of a direct measure of crystal structure of $^{13}$C-enriched CNT. These results are thus not biased by biodistribution of tracers that were detached from the CNT. The detected isotope ratios ($^{13}C/^{12}C$) were related directly to the concentrations of $^{13}$C-SWNT in the various analysed organs; however, the method has a relatively low detection sensitivity (1 ppm) as the presence of natural $^{13}$C is relatively high (1.1% of C).

These results were supported by another study from the same group [25]. Identical SWCNT (L: 2–3 μm, D: 10–30 nm (bundles)) were injected IV in mice. SWCNT were detected by Raman spectroscopy in lung, liver and spleen 90 days post-injection. The intensity was strongest in the lung, and although the analysis was qualitative, the authors noted that the accumulated amounts in the lungs were remarkable. SWCNT were also visible in light microscopy as black spots and by TEM in lysates of liver and lung from the high dose (1 mg/mouse) after 90 days [25].

Unmodified non-commercially available SWCNT (L: 300 nm, D: 1 nm) were injected IV into rabbits (75 μg/animal, 20 μg/kg) and the SWCNT were detected using near-infrared fluorescence [28]. Injected SWCNT were quickly covered with blood proteins, and the blood concentration had a

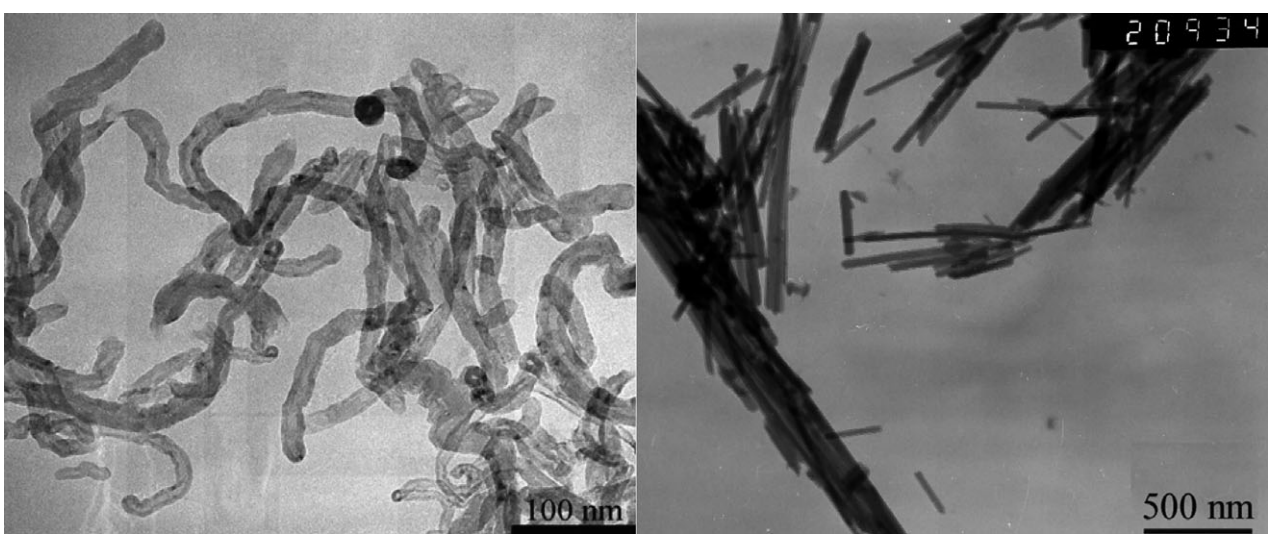


Fig. 3. TEM images of CNT used in oral biodistribution experiments. Left: MWCNT (L: 10–600 nm, D: 10–15 nm). Right: SWCNT (L: 300 nm, D: 1.4 nm (bundles)). Reprinted with permission from J Nanosci. Nanotech. [57] and Carbon [38].

half-life of 1 hr. The experiment was terminated after 24 hr, and SWCNT were clearly detected in the liver as the only of many organs [28].

Classic physiology suggests that once particles are in the blood circulation, there are two common excretion pathways. These are known as renal and the hepatobiliary clearance. Small particles are often excreted in the urine. However, this requires passage through the renal corpuscle with the vast number of perforations (fenestrations/glomerular basement membrane/filtration slits/epithelial podocytes) of the endothelium being <10 nm and with a small subset (<2%) being 15–20 nm [60]. This means that there appears to be a size cut-off point and that larger particles tend to accumulate within the body, primarily within Kupffer cells of the liver. The above-mentioned results support these thoughts. Given the size of these physically large entities made up of agglomerated unmodified particles, they are not excreted but primarily stored in liver tissue as expected. However, the cause for CNT to move from the bloodstream to lung tissue as observed in one of the publications is unknown. However, one hypothesis could be that when injected into circulation via a tail vein, the lung will be the first organ encountered. If CNT agglomerates beyond the diameter of the fine capillaries of the lungs (>2 μm) were injected, these could be trapped and retained in the lung capillaries.

*Modified CNT*. Carbon nanotubes have been proposed as possible carriers for drugs, proteins, peptides and nucleic acids (for gene transfer or gene silencing) and as stable biomolecules in diagnostic applications. For such applications, chemical modifications of the CNT surface may be necessary to target specific organs. Several groups have actively explored this area, and several papers have been published.

*SWCNT*. One study investigated $^{64}$Cu-radiolabelled-DOTA-PEG-SWCNT (L: 100–300 nm, D: 1–5 nm). It was found that small and large PEG chains-SWCNT had blood circulation half-lives of 0.5 and 2 hr, respectively. There was a prominent uptake in the liver and to a much lesser extent spleen and kidney. Larger PEG chain caused a slower blood clearance and lower concentration in liver [48].

A second study using water-soluble and $^{111}$In-labelled SWCNT (L: 0.1–1 μm, D: 1.4 nm) for *in vivo* biodistribution found a fast blood clearance with only 3% and 0.4% of the dose/gram blood after 1 and 20 hr, respectively. Tissue analysis indicated that the major sites of $^{111}$In accumulation were the kidney followed by liver, spleen and, to a much lesser extent, bone. $^{111}$In cleared the kidneys more rapidly than the spleen and liver. Urine was collected 1 hr post-injection and some radioactivity was noted, indicating a possible urine excretion of the tracer [47]. Only their experiments with non-tumour-targeting constructs were considered here.

Carlos Villa and colleagues used SWCNT-$^{111}$In-(DOTA)-coupled to modified DNA oligonucleotides (L: 0.05–0.1 μm, D: ~1–1.5 nm). The results suggested a relatively fast clearance from the blood with 0.4% of the dose/gram blood remaining at 24 hr. SWCNT were mainly located in liver, kidney and spleen. Lower concentration was detected in seven additional organs. The organ radioactivity was relatively similar throughout the experiment (1–96 hr) [41].

Hydroxylated and $^{131}$I-labelled SWCNT (L: 0.3 μm, D: 1.4 nm) were used in a short-term (2-min. to 1-hr) biodistribution study. Radioactivity was found all over the body (except brain) within 2 min. Kidneys, liver, bone, spleen, stomach and lungs were the major target organs in mentioned order. SWCNT in heart, lungs, skin and muscle tissues were correlated with the content in the blood, illustrating both that the bloodstream brings the modified SWCNT to the whole body and that the SWCNT did not accumulate in these tissues. Blood half-life was about 4 min. immediately after the injection and about 50 min. at the end of the experiment (1 hr post-injection) [61].

Kang *et al.* showed blood clearance with a half-life of 3–4 hr, with a concomitant rapid uptake of high levels (~50% of the dose/g) in liver of mice using 488F-chitosan-functionalized SWCNT (before functionalization L: 0.05–0.2 μm, D: 1–3 nm). The amount of accumulated SWCNT in liver did not decrease during the 24-hr period and led to pathological changes such as injury of macrophages, cellular swelling and inflammation and blood coagulation. A similar uptake was observed in spleen and kidney; however, the authors did not observe obvious pathological changes in these organs [27].

Using Raman spectroscopy of SWCNT (L:~100 nm, D: 1–2 nm) non-covalently functionalized by three different lengths of PEG chains (2, 5 and 7 kDa), it was again shown that liver (30–65% of the dose/g tissue) and spleen (19–30% of the dose/gram tissue) are the major sites of accumulation (24 hr) followed by bone, kidney, intestine, stomach and lung. The authors suggested that the majority of CNT accumulate in the liver and renal excretion only occurs for the shortest of the SWCNT. The content of SWCNT in six other tested organs was below the detection limit. Blood circulation time, defined as the time until the blood SWCNT level had dropped to 5% of the dose/gram, was between 1 and 15 hr. The decay rate depended on the modification and size of PEG chains in such a way that functionalization with larger PEG chains increased the circulation time. Additionally, the authors reported a reduced uptake in liver and spleen for largest PEG chain-modified SWCNT compared with the small 2-kDa modified [24]. The results were in line with a previous publication by the same group [48] in which a large-sized PEG chain 5.4 kDa caused a relatively slower blood clearance and concentration in liver than a smaller one of 2 kDa.

PEG1500N-functionalized, acid-treated and thermally annealed SWCNT (L: 0.3–1 μm; D not reported) were administered to mice in order to clarify distribution and biological defunctionalization using Raman and photoluminescence measurements. Only two organs were analysed (liver and spleen) and SWCNT were detected at 1, 4 and 8 weeks post-exposure. Additionally, results suggest that a defunctionalization of the amide linkages between the PEG occurred in the liver (4 and 8 weeks), but not in the spleen [26].

All eight above-mentioned studies included SWCNT with small dimensions (L: <1 μm, D: <2 nm). In seven of them, blood clearance was measured and determined to be relatively

fast. However, the unit was not identical as some use half-life and others the remaining actual dose or a fraction of the injected dose remaining, and yet others a fraction of the dose/g blood at a certain time-point. The half-life varied from a few minutes to several hours depending on the material. The shortest blood half-life (4 min.) was observed with hydroxylated and $^{131}$I-labelled SWCNT (L: 0.3 μm, D: 1.4 nm). This was much shorter than the half-life (4 hr) of an otherwise similar SWCNT (size before functionalization L: 0.05–0.2 μm, D: 1–3 nm) functionalized by adding 3- to 5-kDa biocompatible polymers (chitosan) and green fluorescent dye. The same trend was observed in [24,48] where a larger size of PEG chain was related to increased circulation time and decreased clearance (5% of the dose/gram was between 1 and 15 hr). In two of the papers, kidney followed by liver was mentioned as the primary site of accumulation. In the remaining six papers, liver was the major target organ with much less in spleen and kidney. This distribution was also observed in a study by Schipper *et al.* despite the use of extremely long SWCNT. Mice were injected with oxidized or non-oxidized, non-covalently PEGylated SWCNT (L: 100–300 μm, D: 1–5 nm, oxidized CNT: L: 0.05–0.2 μm). Distribution was determined by histology and Raman spectroscopy. Nanotubes persisted within liver and spleen macrophages until the termination of the experiment 4 months post-exposure without apparent toxicity. There were no changes in survival and clinical parameters of toxicity over the 4 months [23].

Wang *et al.* used hydroxylated SWCNT labelled with $^{125}$I (L: 300 nm, D: 1.4 nm). The distribution pattern of the IV-injected SWCNT mimicked that after the oral exposure described above. The nanotubes moved easily to all compartments and tissues of the body. Highest amounts were detected in stomach, kidney, lungs and bone, and very small amounts were detected in brain. An analysis of the excretion over 11 days demonstrated that about 80% of the total injected radiolabel was collected in faeces and urine (94% in urine and 6% in faeces) [57].

Water-soluble, SWCNT (L: 0.3–1 μm, D: 1 nm) functionalized with DTPA and labelled with indium ($^{111}$In) were used for distribution and imaging analyses [40]. Results indicated that the SWCNT were not retained in organs such as liver and spleen, but were cleared from blood circulation with a half-life of about 3.5 hr through the renal excretion route. At 30 min., largest amounts of $^{111}$In were detected in muscle tissue (49–63% of dose) and skin (8–36% of the dose), whereas at 3 and 24 hr, very low levels were observed in all tested organs. No labelling was observed in the livers. Additionally, DTPA-SWCNT were identified in urine by transmission electron microscopy. In these analyses, it was found that SWCNT primarily existed as bundles of 10–40 tubes (D: 13–40 nm). It is possible that the SWCNT were singular when passing the kidneys and then agglomerated in the urine or during the sample preparation.

SWCNT modified with lysine and DOTA [$^{111}$In](SWCNT-Lys-DOTA[$^{111}$In]) were shown to be excreted in urine after injection in mice. Thirty-four percentage was in the urine after 30 min. Only a smaller percentage remained in the mice after 90 min. (kidneys 1.1% of the dose/g tissue; liver 0.2–0.3% of the dose/g tissue) [44].

Regardless of length, short (100 nm), intermediate (300–1000 nm) or long (100–300 μm), all except three publications [40,44,57] found liver to be the primary site of accumulation. The most common secondary targets were kidney and spleen. It thus points to a distribution profile similar to most small NP [62]. For unmodified SWCNT, lung is also mentioned which may be due to the presence of larger agglomerates (>2 μm). However, it should be noted that the authors did mention agglomerates in the suspension (D: 10–30 nm and L: 2–3 μm), but these appeared to be too small to explain the pulmonary deposition, unless adsorption directly to the endothelium via hydrophobic interactions or needle-like piercing of the membranes is involved [25,30].

According to renal physiology, only very small particles can be excreted in the urine. SWCNT may be much larger than other molecules previously shown unable to pass the kidneys to urine (<30–50 kDa). However, they do have a unique structure that enables just this and thus calls for modifications to the traditional rules for renal filtration. The diameter (thickness) of well-dispersed SWCNT is far below the filtrating size of the renal corpuscle perforations (<10 nm) [60].

McDevitt *et al.* [46] proposed the hypothesis that long, thin SWCNT fibres could negotiate the glomerular filtration on the longitudinal axis (like spaghetti through a sieve). This idea has been further elaborated by Ruggiero in [49]. The authors injected a modified SWCNT (SWCNT-$^{86}$Y-DOTA-AF488-AF680; $D \sim 1$ nm, $100 \leq L \leq 500$ nm, MW: 150–750 kDa) and found that despite these features, $\sim$65% remained within the kidneys 20 min. post-injection. No toxicity or modifications of kidney structure were observed. In addition, the authors provided a theoretical model that suggested that the velocity of the flow at the glomerular perforations (fenestra) ($2 \times 10^{-5}$ m/sec.) is sufficiently high to steer the CNT into the pores in the longitudinal axis. This provides a physical explanation for the observed urine clearance. It should be noted that larger surface modifications may well render the construct less able or even unsuitable for renal clearance. For example, addition of large PEG chains especially with branched structures to the surface of SWCNT altered the PK profiles away from kidney filtration [24].

Table 2 compiles main results from studies using SWCNT labelled with radiotracer attached to DTPA or DOTA. One study showed no difference in distribution profile when DTPA-$^{111}$In is replaced with DOTA-$^{111}$In [43]. Despite the great similarity in exposure conditions, the results vary to a great extent, both in blood clearance and in organ accumulation – from almost all in kidneys and nothing in liver/spleen [40] to the vice versa with most in liver and spleen with less [47] or nothing [48] in kidneys. It should be noted that the latter study used PEGylated SWCNT, which may have caused the reduced kidney filtration. However, still large differences are observed within this group but also when compared to the publications examining distribution of SWCNT with a direct SWCNT detection (Raman, NIR fluorescence and skeleton-enriched SWCNT) all mentioning liver, spleen and lung as

*Table 2.*
Studies using SWCNT with radiotracer-labelled DTPA or DOTA.

| SWCNT | Clearance (blood) | Major sites of deposition | References |
|---|---|---|---|
| DTPA-$^{111}$In | $T_{1/2}$: 3–3.5 hr | **Kidneys.** Much less in skin, liver | [40] |
| DOTA-$^{111}$In | 1 hr: 2.8%ID/g blood<br>20 hr: 0.4%ID/g blood | **Kidneys.** Much less in liver, spleen, bone | [47] |
| DOTA-$^{111}$In | 24 hr: 0.4%ID/g blood | **Liver, kidneys.** Much less in spleen | [41] |
| PEG-DOTA-$^{64}$Cu | $T_{1/2}$: 0.5–2 hr depending on PEG size | **Liver.** Much less in spleen | [48] |
| DOTA-$^{86}$Y | $^{86}$Y cleared at 3 hr | **Liver, spleen.** Less in kidneys, bone | [46] |
| DOTA-$^{86}$Y | $T_{1/2}$: 6 min. | **Kidneys.** Less in liver, spleen | [49] |
| DOTA-$^{111}$In | 34% & 91% in urine after 30 min. and 12 hr | **Kidneys.** Less in liver | [44] |

Bold text indicates a clear major site of deposition. DOTA, 1,4,7,10-tetraazacyclododecane-1,4,7,10-tetraacetic acid; DTPA, diethylen-triamine-penta-acetic dianhydride.

target organs and with no or very limited urinary excretion. One hypothesis might be that three studies used non-covalently PEGylated SWCNT [23,24,26], one used SWCNT non-covalent functionalized with chitosan [27], whereas [28] and [25] used pristine SWCNT, which may have partially agglomerated. Combined, these modifications may have aided in evading kidney filtration. Also, it should be noted that several groups have shown that SWCNT can pass kidney filtration.

*MWCNT.* The distribution of $^{14}$C-tau-MWCNT (10 μg, L: 10–600 nm, D: 10–15 nm) has also been investigated after intravenous injection. Within 10 min., about 80% of the exposed dose had accumulated in the liver. The detected values in liver varied between 75 and 85% through the first month. After 90 days, 20% of the dose was still localized to the liver. TEM images clearly showed MWCNT localized in the Kupffer cells. Smaller amounts (1–5%) were detected in spleen and lung. The results indicated elimination from lung tissue, but a constant or slight build-up in spleen for the 90 days [38].

Taurine-covalently functionalized and Tween-80-wrapped nanotubes labelled with $^{125}$I ($^{125}$I-tau-MWCNT and $^{125}$I-Tween-MWCNT, 10 μg) were dosed IV into mice [33]. After 5 min., about 80% of $^{125}$I-tau-MWCNT was in the liver and smaller amounts in spleen and temporarily in the lung. Liver concentration remained high and ended at 75% of the dose after 6 hr. $^{125}$I-Tween-MWCNT was found to be distributed to the liver, spleen and lung, but also into stomach, kidney, large and small intestine. There were indications that Tween-MWCNT partly evaded liver capture, possible due to dispersion properties of Tween. It should be noted that these results are very similar to those mentioned above by the same group using $^{14}$C-tau-MWCNT [33].

$^{14}$C-MWCNT (L: 3–4 μm, D: ca. 100 nm) was sonicated in pure rat serum until the formation of a stable suspension. After IV delivery in rats, the MWCNT were cleared from the blood (NB: 24 hr was the shortest time-point) and distributed into mainly liver. Lower amounts were detected in lungs, spleen and kidneys, whereas no radioactivity was detected in brain, heart, bones, stomach and muscle (i.e. less than 10 pg in each organ). Optical microscopy revealed dark clusters in lung and liver that coincided with radioactive hot spots. Decreasing radioactivity was observed in all organs over the course of the experiment [32]. This MWCNT experiment should be noted as the C-C covalent bond between CNT and the external $^{14}$C is very strong and much more stable than other radionucleotide complexes used in other studies.

Thick (D: 39.5 nm) and thin (D: 9.2 nm) MWCNT of similar length were surface-modified with amines, whole IgG antibody or the antigen binding region of IgG modified. All contained the radiotracer [$^{111}$In]DTPA. Interestingly, the modifications appeared not to influence the distribution, whereas diameter did. The thick MWCNT were primarily located in spleen and liver with much less in lungs and miniscule amounts in another eight tested organs including kidneys. The narrow MWCNT were primarily located in lungs with less in spleen and liver and far less in heart and kidney and with very low amounts in the remaining organs. The authors suggested that the alveolar macrophages play a role in the increased transport of narrow CNT to lung tissue [45].

Multi-walled carbon nanotubes were aminated and modified with DTPA[$^{111}$In] before being injected into mice. The material accumulated instantly (5 min.) in the lungs (27% of the dose) and liver (19.8% of the dose). Similar concentration was detected throughout the 24-hr period. Low levels (~1–7% of the dose) were detected in skin, spleen, kidneys, muscle and bone. Brain, stomach and heart all had well below 1% of the dose. The blood contained 14% of the dose at 5 min., which decreased at all measuring times to reach 1% of the dose after 24 hr. Body was perfused to avoid [$^{111}$In] signal interference from blood [63].

Al-Jamal *et al.* showed that $^{111}$In-DTPA attached via pyrrolidine amide bonds ($^{111}$In-DTPA-MWCNT) led to about 58–68% distribution to the liver and 2.6–4% in the spleen of the dose. Only very small amounts ended up in the lung and kidneys. Approximately tripling the number of functionalization reduced liver accumulation (42% of the dose) with a concomitant small increase in spleen (5%) and lung (2%). A somewhat increased signal was observed in the bladder for the most functionalized MWCNT compared to the MWCNT with lower levels of functionalization [43].

Multi-walled carbon nanotubes (outer/inner D: 35/10 nm. L: 0.2 μm and up) were oxidized, aminated and loaded with Pt drugs inside the MWCNT. After IV injection, Pt was mainly detected in the livers. When viewed as dose/g tissue, similar levels were detected in liver, kidney, spleen and lung. Some

urine excretion of Pt. MWCNT was verified in liver tissue via microscopy [36].

Water-soluble MWCNT (L: 0.5–2 μm, D: 20–30 nm) functionalized with DTPA and labelled with indium ($^{111}$In) were used for urine excretion studies. DTPA-MWCNT were identified by transmission electron microscopy in the urine. In this analysis, the MWCNT were primarily detected as individual fibres/tubes (D: 30–38 nm) [40]. In another study by the same group, $^{111}$In-labelled DTPA-MWCNT were tracked in rats (size before functionalization: L: 0.5–2 μm, D: 20–30 nm) [42]. Imaging showed that within a minute, the CNT began to accumulate in the kidneys and bladder. At 30 min., most of the detected activity was in the kidneys/bladder. At 6 hr, almost all CNT eliminated via renal excretion route. At 24 hr, only residual levels were detected in liver, spleen, kidneys and bladder. Urinary excretion of the vast majority of radiolabelling (nanotubes) was confirmed at 24 hr, where it was shown that 11.5% of the dose/g tissue was in the urine, whereas the liver, spleen, bladder and kidneys all had content below 1%. Kidney histology (24 hr) showed normal renal morphology without MWCNT accumulation. The rapid urinary clearance of MWCNT observed by Lacerda *et al.* is in contrast to the papers mentioned above. The authors all reported a rapid blood clearance profile predominantly leading to hepatic accumulation. The urinary clearance of MWCNT is also in contrast to the traditional rules for renal filtration (<30–50 kDa), with only a small subset of pores (2%) allowing passage of material up to 20 nm, and to the above-mentioned exception of longitudinal filtration of thin SWCNT, even if the MWCNT were mentioned as being predominantly individualized with average dimensions of 20–30 nm (before functionalization). Smaller dimensions for a subset of the CNT appear not to be a possible explanation as the MWCNT were predominately located in this excretion pathway.

It should be mentioned that Wei *et al.* found 7% of the exposed dose of oxidized and technetium-labelled MWCNT ($^{99m}$Tc-oMWNT, L: 1–10 μm D: 10–30 nm) in collected urine in the first 2 hr after IV exposure. Another 2.6% was detected in the urine between 2 and 25 hr [64]. One other group observed a larger urinary excretion. Guo *et al.* used glucosamine and technetium-modified MWCNT ($^{99m}$Tc-MWNT-G; L: >10 μm, D: 20–40 nm) for intraperitoneal deposition in mice. Activity was mainly located in the urine/faeces of the mice after 24 hr. In the Lacerda and Singh papers, a construct of $^{111}$In-DTPA-MWNT (size before functionalization: L: 0.5–2 μm, D: 20–30) was used [40,42]. However, using the same construct, $^{111}$In-DTPA-MWNT, the same group was not able to reproduce these results in mice as only minor levels were located in the urine and/or kidneys. These include tubes with identical dimensions [63], same diameter, but similar and shorter lengths [43] and tubes with thicker and thinner diameter with similar length [45]. Therefore, the findings on urinary clearance should be reproduced and confirmed. However, it should be emphasized that as several papers/groups now confirm at least small amounts in kidney/urine, the phenomenon should not be ruled out completely, but elaborated and examined further. If excluding those with predominately urine excretion, it appears again that for both SW and MWCNT, liver appeared to be the major target followed by spleen, lung and kidney.

There is no doubt that the different modifications will affect the distribution of IV-injected CNT. Larger side chains may postpone or render urine excretion impossible. Modifications may also improve the CNT dispersibility in physiological and biological compatible media, causing a shift in size towards a suspension of many small agglomerates and individual particles, possibly increasing excretion. It is, however, a major challenge to compare different chemical preparations, functionalizations and study designs. Although the overall distribution changes were not great, it was shown that increasing the level of surface modifications reduced the deposition in the liver from 58 to 68% down to 42% of the dose [43].

*Biological distribution after peritoneal deposition.*

Intraperitoneal injection (IP) is an injection into the body cavity below the diaphragm. IP is rarely used in human beings, but is frequently used in veterinary medicine and in scientific experiments. Only a few papers have described the biological distribution of nanotubes after a peritoneal deposition.

Wang *et al.* have used hydroxylated SWCNT labelled with $^{125}$I [57] and $^{131}$I [61]. The distribution pattern of the IP-injected nanotubes at 3 hr was similar to that observed after oral and IV exposure described above. Highest amounts were detected in stomach, kidney, lungs and bone, and very small amounts were detected in brain. At 6 hr, amounts were highest in stomach, kidney and bone. At 3 and 6 days, nanotubes were only detected in kidney and bone. Very low radiolabelling was detected in all other organs. A large urine excretion was observed within the first 2 days. Eighty percentage was excreted during the first 11 days (94% in urine and 6% in faeces) [57]. In the second study, the hydroxylated $^{131}$I-labelled SWCNT were used in a short-term (2-min. to 1-hr) biodistribution. Radioactivity was found all over the body (except brain) within 2 min. Bone, kidney, stomach, blood, spleen and liver are in mentioned order the major target organs. Lower concentrations were detected in all other organs. Blood half-life was about 4 and 55 min. in the beginning and at end of the experiment, respectively [61].

Another study with functionalized SWCNT (D: 1.4 nm. L: 0.1–1 μm) performed in athymic mice showed a distribution in liver, kidney, spleen and bone with 7.5, 8.5, 9.7 and 1.4% of the dose/g, respectively, after 3 hr and 8.8, 5.4, 7.5 and 1.6% of the dose/g, respectively, after 24 hr. The radioactivity persisted longer in the IP cavity, which seemed to reduce accumulation in liver and spleen. The CNT did not move around the body as similar-sized proteins would [46].

Results by Tsyboulski *et al.* are in contrast to those above. Unmodified SWCNT predominantly accumulated in liver (43 μg/g tissue), spleen (47 μg/g tissue) and kidneys (2.4 μg/g tissue). About 65 μg (38% of the dose) of SWCNT was present in these organs 3 days after SWCNT injection. There was no attempt to measure excretion (urine/faeces) [65].

When using water-soluble MWCNT (L: 10 sec. of μm, D: 20–40 nm) functionalized with glucosamine and labelled with radioactive technetium ($^{99m}$Tc-MWCNT-G), Guo *et al.* showed that blood half-life was 5.5 hr and that CNT moved easily throughout the compartments and tissues of the body. The major organs were the stomach and the enterogastric area. A subsequent excretion experiment (24 hr) showed that about 70% of the activity was collected in urine/faeces. Results indicated that a vast majority of $^{99m}$Tc was bound to MWCNT-G in urine after 24 hr and that there was no free $^{99m}$Tc [39].

Although only few studies on peritoneal exposure have been performed, a distribution pattern starts to form. Unmodified CNT remain in the cavity, but are also engulfed by the liver and possibly spleen. With the exception of [$^{86}$Y]-DOTA-SWCNT [46], modified CNT ($^{125}$I- or $^{131}$I-SWCNT-OH or $^{99m}$Tc-MWCNT-G) appeared to move more freely around the body. Two of the studies (SW and MWCNT) mention large urine excretion. Excretion was not measured in the last, but a large concentration of $^{131}$I was detected in the kidneys.

## Conclusion

Here, we have reviewed the recent studies on *in vivo* biodistribution of CNT. After more than a decade of research, it is clear that a quantitative assessment of the distribution of CNT remains a challenge and largely depends on the development of new and improved detection techniques. Qualitative assessments of CNT deposition in tissues are possible with the present-day techniques, although these can be technically demanding.

Importantly, it has been shown that after pulmonary deposition, CNT remain for months or even years in the lung. The majority of CNT stay in the lung or are cleared via mucociliary escalator towards the GI tract for a second opportunity for uptake. However, there appears to be no uptake of CNT from the GI tract, with the possible exception of functionalized very small SWCNT as shown by one study.

Several groups have reported that a significant fraction of CNT translocate to the near pulmonary region including lymph nodes (<7% of the pulmonary deposited dose), subpleura and pleura (<1%) and to distal organs including liver, spleen and bone marrow (~1%) after deposition of CNT in the airways by inhalation, pharyngeal aspiration or intratracheal instillation. These results clearly demonstrate the main sites of CNT accumulation, which include pleura, a major site for fibre-induced pulmonary diseases.

To locate other sites of accumulation, larger CNT exposures can be dosed via, for example, IV injection. A large number of studies have explored the biodistribution of pristine or functionalized CNT after IV injection. Although this is a pharmacologically relevant exposure route, it should be considered that the material enters circulation at different sites.

Unmodified CNT administered IV have a clear preference for liver and lung. The hepatic uptake is similar to that observed for the majority of NP and is in compliance with the traditional blood clearance pathway of solid materials. As shown by several groups, small particles (such as surface-modified SWCNT) can be excreted in the urine. Larger particles or agglomerates may be taken by Kupffer cells in the liver. One possible mechanism for the CNT to deposit and concentrate in the lung is that when injected into circulation via a tail vein, the lung will be the first organ capillary network encountered. If some of the injected CNT agglomerates are larger than the diameter of the fine capillaries of the lungs (>2 μm), these may be trapped and retained in the lung. Another possibility is that highly hydrophobic materials (such as pristine CNT) may adhere strongly to the endothelium of capillary network.

In general, IV injection studies have shown ample evidence that CNT in blood circulation are cleared relatively fast with a half-life of minutes or hours. Some functionalizations alter the blood circulation time. The primary target organs for IV-injected SWCNT are the liver with the most common secondary targets being kidney and spleen. For modified SWCNT, kidney and urine excretion has been shown by several groups. For MWCNT, the primary target is liver followed by spleen, lung and kidney.

There is no doubt that functionalizations can either increase or decrease the urinary excretion and that specific targeting moiety can direct CNT to specific cell types. But the overwhelming body of evidence shows that nanotubes without such moieties will primarily be distributed to the liver where they can stay for a long time. Several different kinds of CNT have been observed in the liver up to 1 year after exposure.

In the present MiniReview, the biodistribution and biological durability of CNT are discussed. The above-mentioned results clearly show that CNT deposited in the lung translocate to pleura and lymph nodes near the lung but also to distal organs including liver and spleen – presumably via circulation. Clearing rates appear to be very low. IV injections confirm these primary targets, but additionally secondary targets including lung and kidney are added. With the limited data available, there appears not to be any uptake from the GI tract of CNT. The consequence of translocation and CNT accumulation in, for example, pleura, liver and spleen is presently unknown, but is of great concern. Still, too little is known about the influence of physical and chemical parameters on the biodistribution and toxicity, and further research in this area is of paramount importance.

### Acknowledgements

This work was supported by The Danish DFF (Grant No 6110-00103), The European Union FP7 (Grant No 310584; NANoREG and Grant No 263147; NanoValid), the Danish Centre for Nanosafety II and the Danish EPA J.No. 1805.

### Conflict of Interest

The authors declare no conflict of interest.

## References

1 Jensen KA, Bøgelund J, Jackson P, Jacobsen NR, Birkedal R, Clausen PA *et al.* Carbon Nanotubes – Types, Products, Market and Provisional Assessment of the Associated Risks to Man and the Environment. Environmental Project No. 1805, 2015.

2 Markets and Markets. Carbon Nanotubes Market by Type (Single Walled- And Multi Walled) – Global Forecasts to 2020. 2015.
3 Møller P, Jacobsen NR, Folkmann JK, Danielsen PH, Mikkelsen L, Hemmingsen JG *et al.* Role of oxidative damage in toxicity of particulates. Free Radic Res 2010;**44**:1–46.
4 Johnston H, Pojana G, Zuin S, Jacobsen NR, Møller P, Loft S *et al.* Engineered nanomaterial risk. Lessons learnt from completed nanotoxicology studies: potential solutions to current and future challenges. Crit Rev Toxicol 2013;**43**:1–20.
5 Donaldson K, Poland CA, Murphy FA, MacFarlane M, Chernova T, Schinwald A. Pulmonary toxicity of carbon nanotubes and asbestos – similarities and differences. Adv Drug Deliv Rev 2013;**65**:2078–86.
6 Rom WN, Travis WD, Brody AR. Cellular and molecular basis of the asbestos-related diseases. Am Rev Resp Dis 1991;**143**:408–22.
7 Møller P, Christophersen DV, Jensen DM, Kermanizadeh A, Roursgaard M, Jacobsen NR *et al.* Role of oxidative stress in carbon nanotube-generated health effects. Arch Toxicol 2014;**88**:1939–64.
8 Jackson P, Jacobsen NR, Baun A, Birkedal R, Kuhnel D, Jensen KA *et al.* Bioaccumulation and ecotoxicity of carbon nanotubes. Chem Cent J 2013;**7**:154.
9 Grosse Y, Loomis D, Guyton KZ, Lauby-Secretan B, El GF, Bouvard V *et al.* Carcinogenicity of fluoro-edenite, silicon carbide fibres and whiskers, and carbon nanotubes. Lancet Oncol 2014;**15**:1427–8.
10 Ma-Hock L, Treumann S, Strauss V, Brill S, Luizi F, Mertler M *et al.* Inhalation toxicity of multiwall carbon nanotubes in rats exposed for 3 months. Toxicol Sci 2009;**112**:468–81.
11 Pauluhn J. Subchronic 13-week inhalation exposure of rats to multiwalled carbon nanotubes: toxic effects are determined by density of agglomerate structures, not fibrillar structures. Toxicol Sci 2010a;**113**:226–42.
12 Pauluhn J. Multi-walled carbon nanotubes (Baytubes): approach for derivation of occupational exposure limit. Regul Toxicol Pharmacol 2010b;**57**:78–89.
13 Poulsen SS, Saber AT, Mortensen A, Szarek J, Wu D, Williams A *et al.* Changes in cholesterol homeostasis and acute phase response link pulmonary exposure to multi-walled carbon nanotubes to risk of cardiovascular disease. Toxicol Appl Pharmacol 2015a;**283**:210–22.
14 Poulsen SS, Saber AT, Williams A, Andersen O, Kobler C, Atluri R *et al.* MWCNTs of different physicochemical properties cause similar inflammatory responses, but differences in transcriptional and histological markers of fibrosis in mouse lungs. Toxicol Appl Pharmacol 2015b;**284**:16–32.
15 Nikota J, Williams A, Yauk CL, Wallin H, Vogel U, Halappanavar S. Meta-analysis of transcriptomic responses as a means to identify pulmonary disease outcomes for engineered nanomaterials. Part Fibre Toxicol 2016;**13**:25.
16 Poulsen SS, Jackson P, Kling K, Knudsen KB, Skaug V, Kyjovska ZO *et al.* Multi-walled carbon nanotube physicochemical properties predict pulmonary inflammation and genotoxicity. Nanotoxicology 2016;**10**:1263–75.
17 Serpell CJ, Kostarelos K, Davis BG. Can carbon nanotubes deliver on their promise in biology? Harnessing unique properties for unparalleled applications. ACS Cent Sci 2016;**2**:190–200.
18 Lee JH, Lee SB, Bae GN, Jeon KS, Yoon JU, Ji JH *et al.* Exposure assessment of carbon nanotube manufacturing workplaces. Inhal Toxicol 2010;**22**:369–81.
19 Han JH, Lee EJ, Lee JH, So KP, Lee YH, Bae GN *et al.* Monitoring multiwalled carbon nanotube exposure in carbon nanotube research facility. Inhal Toxicol 2008;**20**:741–9.
20 Købler C, Poulsen SS, Saber AT, Jacobsen NR, Wallin H, Yauk CL *et al.* Time-dependent subcellular distribution and effects of carbon nanotubes in lungs of mice. PLoS One 2015;**10**:e0116481.
21 Mercer RR, Scabilloni JF, Hubbs AF, Wang L, Battelli LA, McKinney W *et al.* Extrapulmonary transport of MWCNT following inhalation exposure. Part Fibre Toxicol 2013;**10**:38.
22 Ingle T, Dervishi E, Biris AR, Mustafa T, Buchanan RA, Biris AS. Raman spectroscopy analysis and mapping the biodistribution of inhaled carbon nanotubes in the lungs and blood of mice. J Appl Toxicol 2013;**33**:1044–52.
23 Schipper ML, Nakayama-Ratchford N, Davis CR, Kam NW, Chu P, Liu Z *et al.* A pilot toxicology study of single-walled carbon nanotubes in a small sample of mice. Nat Nanotechnol 2008;**3**:216–21.
24 Liu Z, Davis C, Cai W, He L, Chen X, Dai H. Circulation and long-term fate of functionalized, biocompatible single-walled carbon nanotubes in mice probed by Raman spectroscopy. Proc Natl Acad Sci USA 2008;**105**:1410–5.
25 Yang ST, Wang X, Jia G, Gu Y, Wang T, Nie H *et al.* Long-term accumulation and low toxicity of single-walled carbon nanotubes in intravenously exposed mice. Toxicol Lett 2008;**181**:182–9.
26 Yang ST, Wang H, Meziani MJ, Liu Y, Wang X, Sun YP. Biodefunctionalization of functionalized single-walled carbon nanotubes in mice. Biomacromolecules 2009;**10**:2009–12.
27 Kang B, Yu D, Dai Y, Chang S, Chen D, Ding Y. Biodistribution and accumulation of intravenously administered carbon nanotubes in mice probed by Raman spectroscopy and fluorescent labeling. Carbon 2009;**47**:1189–92.
28 Cherukuri P, Gannon CJ, Leeuw TK, Schmidt HK, Smalley RE, Curley SA *et al.* Mammalian pharmacokinetics of carbon nanotubes using intrinsic near-infrared fluorescence. Proc Natl Acad Sci USA 2006;**103**:18882–6.
29 Welsher K, Sherlock SP, Dai H. Deep-tissue anatomical imaging of mice using carbon nanotube fluorophores in the second near-infrared window. Proc Natl Acad Sci USA 2011;**108**:8943–8.
30 Yang S, Guo W, Lin Y, Deng X, Wang H, Sun H *et al.* Biodistribution of pristine single-walled carbon nanotubes in vivo. J Phys Chem C 2007;**111**:17761–4.
31 Czarny B, Georgin D, Berthon F, Plastow G, Pinault M, Patriarche G *et al.* Carbon nanotube translocation to distant organs after pulmonary exposure: insights from in situ (14)C-radiolabeling and tissue radioimaging. ACS Nano 2014;**8**:5715–24.
32 Georgin D, Czarny B, Botquin M, Mayne-L'hermite M, Pinault M, Bouchet-Fabre B *et al.* Preparation of (14)C-labeled multiwalled carbon nanotubes for biodistribution investigations. J Am Chem Soc 2009;**131**:14658–9.
33 Deng X, Yang S, Nie H, Wang H, Liu Y. A generally adoptable radiotracing method for tracking carbon nanotubes in animals. Nanotechnology 2008;**19**:075101.
34 Lin Z, Zhang H, Huang J, Xi Z, Liu L, Lin B. Biodistribution of single-walled carbon nanotubes in rats. Toxicol Res 2014;**3**:497–592.
35 Elgrabli D, Floriani M, Bella-Gallart S, Meunier L, Gamez C, Delalain P *et al.* Biodistribution and clearance of instilled carbon nanotubes in rat lung. Part Fibre Toxicol 2008;**5**:20.
36 Li J, Pant A, Chin CF, Ang WH, Menard-Moyon C, Nayak TR *et al.* In vivo biodistribution of platinum-based drugs encapsulated into multi-walled carbon nanotubes. Nanomedicine 2014;**10**:1465–75.
37 Nakamura M, Tahara Y, Murakami T, Iilima S, Yudasaka M. Gastrointestinal actions of orally-administered single-walled carbon nanohorns. Carbon 2014;**69**:409–16.
38 Deng X, Jia G, Wang H, Sun H, Wang X, Yang S *et al.* Translocation and fate of multi-walled carbon nanotube in vivo. Carbon 2007;**45**:1419–24.
39 Guo J, Zhang X, Li Q, Li W. Biodistribution of functionalized multiwall carbon nanotubes in mice. Nucl Med Biol 2007;**34**:579–83.

40 Singh R, Pantarotto D, Lacerda L, Pastorin G, Klumpp C, Prato M *et al.* Tissue biodistribution and blood clearance rates of intravenously administered carbon nanotube radiotracers. Proc Natl Acad Sci USA 2006;**103**:3357–62.
41 Villa CH, McDevitt MR, Escorcia FE, Rey DA, Bergkvist M, Batt CA *et al.* Synthesis and biodistribution of oligonucleotide-functionalized, tumor-targetable carbon nanotubes. Nano Lett 2008;**8**:4221–8.
42 Lacerda L, Bianco A, Prato M, Kostarelos K. Carbon nanotubes as nanomedicines: from toxicology to pharmacology. Adv Drug Deliv Rev 2006;**58**:1460–70.
43 Al-Jamal KT, Nunes A, Methven L, li-Boucetta H, Li S, Toma FM *et al.* Degree of chemical functionalization of carbon nanotubes determines tissue distribution and excretion profile. Angew Chem Int Ed Engl 2012;**51**:6389–93.
44 Mulvey JJ, Feinberg EN, Alidori S, McDevitt MR, Heller DA, Scheinberg DA. Synthesis, pharmacokinetics, and biological use of lysine-modified single-walled carbon nanotubes. Int J Nanomed 2014;**9**:4245–55.
45 Wang JT, Fabbro C, Venturelli E, Menard-Moyon C, Chaloin O, Da RT *et al.* The relationship between the diameter of chemically-functionalized multi-walled carbon nanotubes and their organ biodistribution profiles in vivo. Biomaterials 2014;**35**:9517–28.
46 McDevitt MR, Chattopadhyay D, Jaggi JS, Finn RD, Zanzonico PB, Villa C *et al.* PET imaging of soluble yttrium-86-labeled carbon nanotubes in mice. PLoS One 2007a;**2**:e907.
47 McDevitt MR, Chattopadhyay D, Kappel BJ, Jaggi JS, Schiffman SR, Antczak C *et al.* Tumor targeting with antibody-functionalized, radiolabeled carbon nanotubes. J Nucl Med 2007b;**48**:1180–9.
48 Liu Z, Cai W, He L, Nakayama N, Chen K, Sun X *et al.* In vivo biodistribution and highly efficient tumour targeting of carbon nanotubes in mice. Nat Nanotechnol 2007;**2**:47–52.
49 Ruggiero A, Villa CH, Bander E, Rey DA, Bergkvist M, Batt CA *et al.* Paradoxical glomerular filtration of carbon nanotubes. Proc Natl Acad Sci USA 2010;**107**:12369–74.
50 Shinohara N, Nakazato T, Ohkawa K, Tamura M, Kobayashi N, Morimoto Y *et al.* Long-term retention of pristine multi-walled carbon nanotubes in rat lungs after intratracheal instillation. J Appl Toxicol 2016;**36**:501–9.
51 Ellinger-Ziegelbauer H, Pauluhn J. Pulmonary toxicity of multi-walled carbon nanotubes (Baytubes) relative to alpha-quartz following a single 6 h inhalation exposure of rats and a 3 months post-exposure period. Toxicology 2009;**266**:16–29.
52 Ryman-Rasmussen JP, Cesta MF, Brody AR, Shipley-Phillips JK, Everitt JI, Tewksbury EW *et al.* Inhaled carbon nanotubes reach the subpleural tissue in mice. Nat Nanotechnol 2009;**4**:747–51.
53 Mercer RR, Hubbs AF, Scabilloni JF, Wang L, Battelli LA, Schwegler-Berry D *et al.* Distribution and persistence of pleural penetrations by multi-walled carbon nanotubes. Part Fibre Toxicol 2010;**7**:28.
54 Porter DW, Hubbs AF, Mercer RR, Wu N, Wolfarth MG, Sriram K *et al.* Mouse pulmonary dose- and time course-responses induced by exposure to multi-walled carbon nanotubes. Toxicology 2010;**269**:136–47.
55 Køhler C, Saber AT, Jacobsen NR, Wallin H, Vogel U, Qvortrup K *et al.* FIB-SEM imaging of carbon nanotubes in mouse lung tissue. Anal Bioanal Chem 2014;**406**:3863–73.
56 Kagan VE, Konduru NV, Feng W, Allen BL, Conroy J, Volkov Y *et al.* Carbon nanotubes degraded by neutrophil myeloperoxidase induce less pulmonary inflammation. Nat Nanotechnol 2010;**5**:354–9.
57 Wang H, Wang J, Deng X, Sun H, Shi Z, Gu Z *et al.* Biodistribution of carbon single-wall carbon nanotubes in mice. J Nanosci Nanotechnol 2004;**4**:1019–24.
58 Yang K, Gong H, Shi X, Wan J, Zhang Y, Liu Z. In vivo biodistribution and toxicology of functionalized nano-graphene oxide in mice after oral and intraperitoneal administration. Biomaterials 2013;**34**:2787–95.
59 Geraets L, Oomen AG, Krystek P, Jacobsen NR, Wallin H, Laurentie M *et al.* Tissue distribution and elimination after oral and intravenous administration of different titanium dioxide nanoparticles in rats. Part Fibre Toxicol 2014;**11**:30.
60 Haraldson B, Sörensson J. Why do we not all have proteinuria? An update of our current understanding of the glomerular barrier. Physiology 2016;**19**:7–10.
61 Wang J, Deng X, Yang S, Wang H, Zhao Y, Liu Y. Rapid translocation and pharmacokinetics of hydroxylated single-walled carbon nanotubes in mice. Nanotoxicology 2008;**2**:28–32.
62 Kermanizadeh A, Balharry D, Wallin H, Loft S, Moller P. Nanomaterial translocation–the biokinetics, tissue accumulation, toxicity and fate of materials in secondary organs–a review. Crit Rev Toxicol 2015;**45**:837–72.
63 Kafa H, Wang JT, Rubio N, Venner K, Anderson G, Pach E *et al.* The interaction of carbon nanotubes with an in vitro blood-brain barrier model and mouse brain in vivo. Biomaterials 2015;**53**:437–52.
64 Wei Q, Zhan L, Juanjuan B, Jing W, Jianjun W, Taoli S *et al.* Biodistribution of co-exposure to multi-walled carbon nanotubes and nanodiamonds in mice. Nanoscale Res Lett 2012;**7**:473.
65 Tsyboulski DA, Liopo AV, Su R, Ermilov SA, Bachilo SM, Weisman RB *et al.* Enabling in vivo measurements of nanoparticle concentrations with three-dimensional optoacoustic tomography. J Biophotonics 2014;**7**:581–8.

## Supporting Information

Additional Supporting Information may be found online in the supporting information tab for this article:

**Table S1.** Experiments on the biological distribution of SWCNT (Top) and MWCNT (Bottom) in animals.